

Total Reflection X-ray Fluorescence—An Efficient Method for Micro-, Trace and Surface Layer Analysis*

Invited Lecture

Reinhold Klockenkämper and Alex von Bohlen

Institut für Spektrochemie und angewandte Spektroskopie, P.O. Box 10 13 52, W-4600 Dortmund, Germany

Total reflection X-ray fluorescence spectrometry (TXRF) uses an ingenious excitation technique for energy-dispersive X-ray spectral analysis. A minute amount of sample is placed on an optically flat carrier and irradiated at a grazing incidence (an angle of only a few minutes) so that the carrier totally reflects the primary beam. The method is particularly suitable for micro-, trace and surface layer analysis. Microanalysis can be performed because $<1 \mu\text{g}$ of a solid sample or $<10 \mu\text{l}$ of a solution are required. Trace analyses are based on detection limits at the picogramme level and can be applied to aqueous solutions (1 pg ml^{-1}), acids (10 pg ml^{-1}), biological materials (10 ng ml^{-1}) and ultra-pure metals (10 ng g^{-1}) after matrix separation. A simple and reliable quantification can be carried out by the addition of an internal standard element. Surface and thin-film analyses are applied to semiconductor wafer materials. Contaminations at $1 \times 10^{10} \text{ atoms cm}^{-2}$ can be detected and even nanometre thick layers can be investigated by non-destructive depth profiling. For this latter purpose, the angle of incidence is continuously varied in the range of total reflection and an angle-dependent intensity profile is recorded.

Keywords: Total reflection X-ray fluorescence; energy-dispersive analysis; microanalysis; trace analysis; surface layer analysis

Within the last three decades, X-ray fluorescence spectrometry (XRF) has become a well-known method of instrumental analysis. It plays an important role in the industrial production of materials, in prospecting mineral resources and, recently, in environmental control. The number of instruments in use are estimated to be about 15 000 worldwide. However, although the method might be extremely good, an important advance was made by an ingenious excitation technique using total reflection for XRF (TXRF). Yoneda and Horiuchi proposed the technique in 1971,¹ and subsequently, Wobrauschek and Aiginger presented the first applications and described the physical principles.^{2,3} In 1980, Schwenke and Knoth developed a compact instrument of high stability, including an additional total-reflection filter.⁴⁻⁶ This instrument, Extra II, is supplied by Rich. Seifert, Ahrensburg, Germany. Other instruments such as the XSA 8000 and TXRF 8010, which are especially suited for wafer analysis, are commercially available from Atomica, Munich, Germany (a subsidiary of Perkin-Elmer). For about 3 years, the Trex 600 has been supplied by Technos, Osaka, Japan and the Model 3726 by Rigaku, Osaka, Japan. Workshops on TXRF took place in 1986, 1988 and 1990 and the papers presented have subsequently been published.⁷⁻⁹ A great variety of applications have already promoted the growing interest in TXRF and the considerable advantages of the technique will make it a well-established method of instrumental analysis in the near future.

Principles

Although TXRF is a variation of XRF and is based on the same characteristic principles it has one significant difference. As is illustrated in Fig. 1, the primary beam strikes the sample not at an angle of about 40° but at only a few minutes. Coming from a line focus X-ray tube and shaped like a strip of paper with its long axis in the horizontal

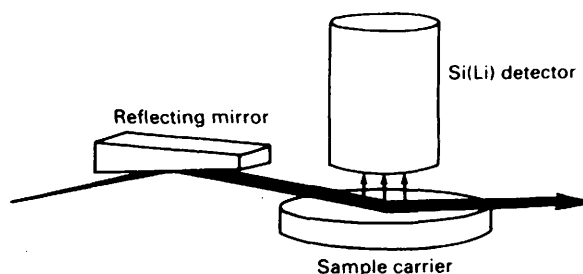


Fig. 1 Simplified instrumental set-up for TXRF. The reflecting mirror can be a low-pass filter or Bragg monochromator. A limited amount and thickness of sample is placed on the carrier

plane, it is at first directed at a totally-reflecting or a Bragg-reflecting mirror. After selective filtration or even monochromatization, it hits the sample carrier at a glancing angle of about 4 min . Owing to this grazing incidence, the beam is totally reflected at the carrier surface. The trace amount of sample, placed on the carrier, is passed through by the primary and by the totally-reflected beam and is excited to X-ray fluorescence. The emitted radiation is detected by a Si(Li) detector, mounted directly above the sample, and recorded as an energy-dispersive spectrum.

A number of materials are suitable as sample carriers. In addition to polished quartz glass, germanium, glassy carbon or the low-cost plexiglass (Perspex) can be used. Of course, the carriers must be optically flat and extremely clean.

Total Reflection of X-rays

When radiation travels from one medium to another with a smaller refractive index, the phenomenon of total reflection can occur. In particular, for X-rays, any medium has a smaller refractive index than air so that total reflection is generally possible although the glancing angles might be small.

* Presented at the XXVII Colloquium Spectroscopicum Internationale (CSI), Bergen, Norway, June 9-14, 1991.

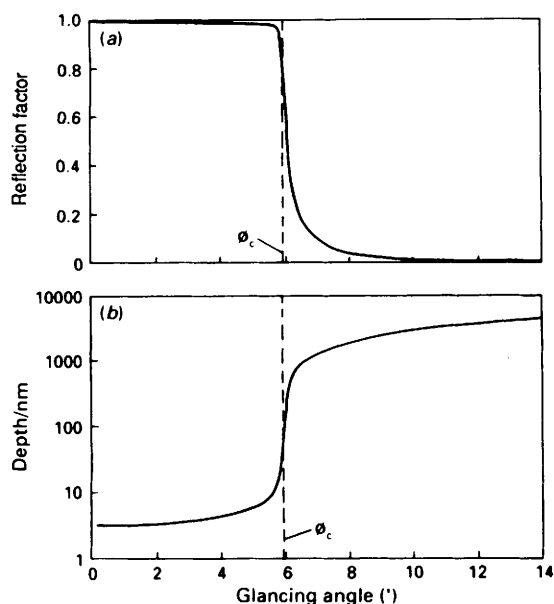


Fig. 2 (a) Reflection factor and (b) penetration depth for Mo K α X-rays and quartz glass, depending on the angle of incidence (in minutes). The critical angle of total reflection is ϕ_c .

For absorptive media the refractive index (n) is given by a complex quantity

$$n = 1 - \delta - i \times \beta \tag{1}$$

where i is the square root of -1 .

The real component δ , called decrement, is a measure of the dispersion and, for X-rays, is of the order of 1×10^{-6} . The imaginary component, β , is a measure of the absorption is even smaller for many media. Both quantities can be reduced to physical parameters:

$$\delta = \frac{N_A}{2\pi} \times r_0 \times \frac{\sum Z_i}{\sum A_i} \times \rho \times \lambda^2 \tag{2}$$

$$\beta = \frac{\lambda}{4\pi} \times \left(\frac{\mu}{\rho}\right) \times \rho \tag{3}$$

where N_A indicates Avogadro's number, r_0 , the classical electron radius (2.818×10^{-13} cm), Z_i , the atomic number and A_i , the relative atomic mass of the element fractions (i) of the reflector material and ρ is its density; (μ/ρ) is the mass absorption coefficient and λ the wavelength of radiation. Total reflection of X-rays occurs for very small glancing angles. For transparent media, for which $\beta/\delta \approx 0$, there is a very distinct limit, the so-called critical angle, ϕ_c . It can be calculated according to Snell's law

$$\phi_c = \sqrt{2\delta} \tag{4}$$

For K α X-rays of Mo striking quartz glass, $\delta = 1.5 \times 10^{-6}$, $\beta = 4.6 \times 10^{-9}$ and $\phi_c = 1.73$ mrad or 5.9 min.

Above all, total reflection is characterized by high reflectivity and consequently, low penetration depth. Both quantities can be calculated by formulae¹⁰ depending on the glancing angle, ϕ . Fig. 2 illustrates the situation for Mo radiation reflected on quartz glass. The reflection factor sharply increases from less than 0.3 to about 100%, whereas the penetration depth sharply decreases from some micrometres to 3.3 nm if ϕ becomes zero.

For spectral analyses, total reflection of the primary beam results in a considerable reduction of the background intensity (I_B) and a duplication of the line intensity (Fig. 3). The background is mainly caused by the Rayleigh and

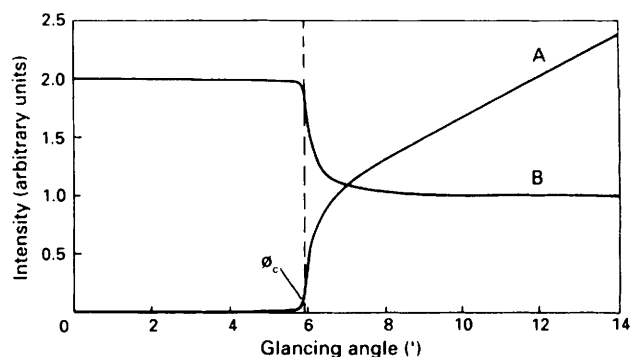


Fig. 3 Intensity of A, background and B, spectral line depending on the angle of incidence (in minutes) at which the Mo K α -beam is striking the sample

Compton scattering of the primary beam at the carrier and is proportional to

$$I_B \propto \sin\phi \times (1-R) \tag{5}$$

where R is the reflection factor. At larger angles, the background follows the well-known $\sin\phi$ law, but at the critical angle, it is drastically reduced according to $(1-R)$.

The sample on top of the carrier is excited to fluorescence by the incident beam and its reflected part. Consequently, the line intensity (I_L) is determined by

$$I_L \propto (1+R) \tag{6}$$

and is nearly doubled beyond the critical angle. The detection power depending on the signal-to-noise (S/N) ratio could be improved by the factor $I_L/\sqrt{I_B}$, which is equivalent to an improvement of about three orders of magnitude.

Experimental Requirements for TXRF

In order to achieve the predicted improvement, some conditions have to be met. The primary beam has to be directed towards the carrier at the grazing incidence. Under the adjusted angle, ϕ_0 (for example, 4 min), the Mo radiation is totally reflected in addition to the longer wavelength part of the Bremsstrahlung. However, the shorter wavelength part would not be totally reflected under this angle. It would penetrate into the carrier and cause a significant background. The undesired part of the primary spectrum is determined by combining eqns. (2) and (4):

$$\lambda \leq 0.0177 \times \frac{\phi_0}{\sqrt{\rho}} \tag{7}$$

or, respectively,

$$E \geq 70 \times \frac{\sqrt{\rho}}{\phi_0} \tag{8}$$

where ϕ_0 is the adjusted angle (in min), ρ is the density of the carrier (in g cm^{-3}), λ is the wavelength (in nm) and E is the energy (in keV). If quartz glass is the carrier and $\phi_0 = 4$ min, X-rays with energies of greater than 27 keV are not subject to total reflection.

In order to avoid the background, which results from this considerable part of the Bremsstrahlung, a special cut-off filter is used. For this reason, an additional quartz reflector^{11,12} is positioned in front of the quartz carrier (Fig. 1). It absorbs the high-energy radiation but totally reflects the Mo and low-energy radiation under the angle ϕ_0 . The cut-off filter is best suited for efficient excitation. Another effective filter is based on a Bragg monochromator¹³ or on a synthetic multi-layer. The relevant glancing angles are more

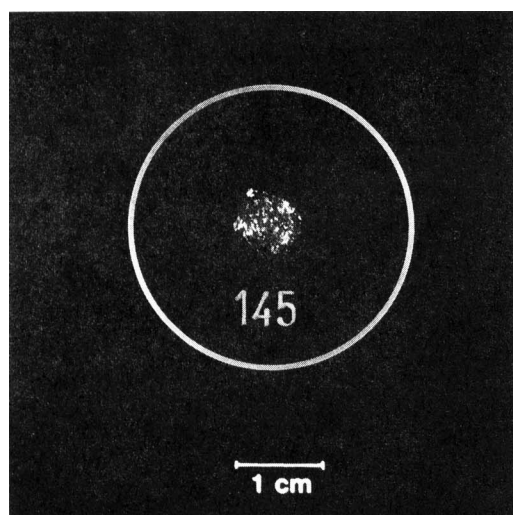


Fig. 4 Dry residue of a 10 μl droplet of suspension on a carrier of quartz glass

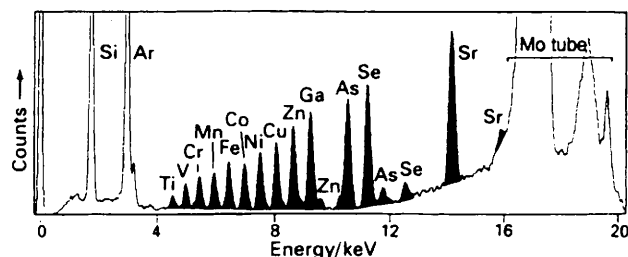


Fig. 5 TXRF spectrum of a silicon disc loaded with a multi-element standard. A droplet of 20 μl with a concentration of 15 $\mu\text{g l}^{-1}$ for each element was pipetted onto the disc and dried

convenient and the main spectral line of the X-ray tube can be selected on its own.

A further condition is related to the sample, which has to be deposited on the carrier so that total reflection can occur without any or with only a little disruption. As a first example, a droplet of a solution or suspension can be pipetted onto the carrier and dried by evaporation. In order to avoid bleeding of the droplet, the carrier can be covered by a hydrophobic film prior to use, for example, one consisting of a silicone compound. The granular residue of such a droplet is shown in Fig. 4. Secondly, a few grains of pulverized material can be used, and thirdly, thin sections of biological materials are also possible. At any rate, the sample must be thin and rough so that it does not take part in the process of total reflection. Furthermore, the sample has to be restricted to the field of vision of the detector, which is generally a circle of 6–8 mm in diameter.

Analytical Features

A multi-element TXRF spectrum displaying the number of accumulated counts versus the energy of X-ray photons is shown in Fig. 5. The Si peak originates from the quartz glass carrier but can be avoided if either glassy carbon or Perspex is used. The Ar peak is a result of air in the gap between the carrier and the detector and can be suppressed by flooding the space with nitrogen. The Mo peaks above 16 keV originate from the Mo anode of the X-ray tube, but the region below these peaks, which are unavoidable, shows the very low spectral background that is an important characteristic of TXRF.

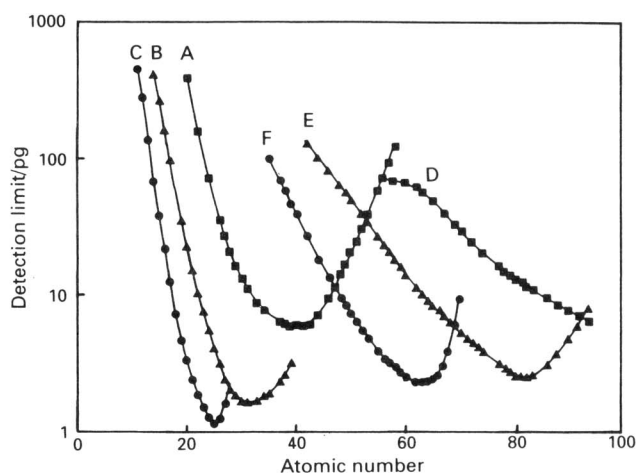


Fig. 6 Detection limits (3σ values) of TXRF for the residues of aqueous solutions.¹⁴ Different excitation modes were used: A and D, W tube (60 kV), Ni filter, cut-off 35 keV; B and E, Mo tube (60 kV), Mo filter, cut-off 20 keV; and C and F, W tube (25 kV), Cu filter. A, B and C are determined by K-lines, and D, E and F by L-lines

The cleaned carrier was loaded with 20 μl of an aqueous standard solution. The spectrum shows the K peaks of 13 elements resulting from only 300 pg of these elements. The multi-element spectrum illustrates the simultaneous determination of the elements and also the high but different sensitivities.

Detection Limits

The improved S/N ratio leads to correspondingly low detection limits¹⁴ as presented in Fig. 6, which shows a clear relationship to the atomic number of the respective analyte. The values were measured with the residues of aqueous standard solutions using a counting time of 1000 s. The actual elapsed time was about 1200 s or 20 min owing to a dead-time correction. The Si(Li) detector that was used had an effective area of 80 mm² and a spectral resolution of 150 eV (full width at half maximum; FWHM) for the Mn K α -line.

Three excitation modes, easily achievable using the twin source of the Seifert Extra II instrument equipped with both a W and a Mo tube, were used. (i) A W tube was combined with a cut-off filter, set at 35 keV, to excite the heavy elements by the continuous spectrum. The interfering W L-lines were suppressed by an additional Ni filter. (ii) A Mo tube was used with a cut-off filter, set at 20 keV, for excitation of the medium elements by the Mo K-lines. In both (i) and (ii), the X-ray tubes were operated at 60 kV and 30 mA. (iii) The Ni filter in (i) was replaced by a Cu filter and the operating voltage was reduced to 25 kV to excite the light elements by the W L-lines more efficiently.

These three excitation modes were used to detect the total range of elements with atomic numbers above 11 (Na). The elements are detectable down to the low picogramme level, either by their K- or L-lines. Consequently, the nanogram per gram level is reached if 100 μg of an organic matrix are applied, and even the nanogram per litre region if 100 μl of a high-purity water or acid are used. Elements lighter than Na can be detected if diamond-like carbon windows, only 0.4 μm thick, are used for the detector, or even windowless detectors and vacuum chambers.^{15,16}

Quantification

Besides detection power, a further advantage of TXRF is the simple and reliable quantification. Samples, deposited

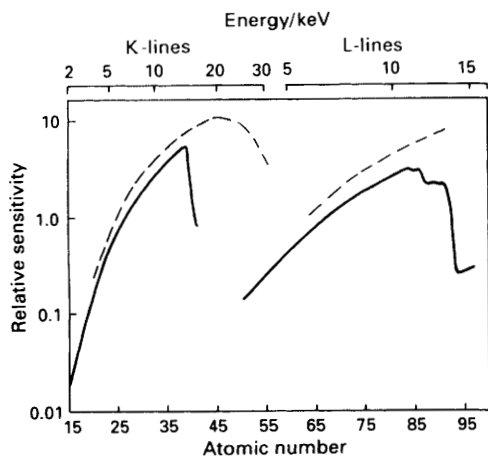


Fig. 7 Relative sensitivity of elements, depending on their atomic numbers, for excitation with a W tube (broken lines)¹⁷ and a Mo tube (solid lines).¹⁸ The upper abscissa displays the energy of the respective K- or L-lines

as thin specimens, do not show any matrix effects so calibration can be based on straight lines, which are independent of the matrix. The slope or sensitivity is solely dependent on the respective element.

For this reason, quantification can be carried out by simply adding some of the standard element to the sample, which previously did not contain any of this particular element. Henceforth, it serves as an internal standard. The unknown concentration of any other element can be calculated by the simple equation:

$$c_x = \frac{N_x/S_x}{N_i/S_i} \times c_i \quad (9)$$

where c indicates the concentration, N the net intensity and S the relative sensitivity of either the analyte, x , or of the internal standard, i . Only a single internal standard element is needed even for multi-element analyses over a dynamic range of more than three orders of magnitude. This standard element can even be added after the sample has been placed on the carrier.

The sensitivity values, S , have to be carefully determined, which, in general, is only done after the installation and the repair or modification of an instrument. If similar instruments are used, the values can even be transferred. Fig. 7 shows the relative sensitivities measured at the K- and L-lines of the different analytes after excitation with a W or a Mo tube.^{17,18}

The Mo curves were actually calculated using only three fundamental parameters:¹⁸

$$S \propto \omega \times \frac{1-r}{r} \times \left(\frac{\mu}{\rho} \right) \quad (10)$$

where ω is the fluorescence yield, r is the jump ratio at the absorption edge and (μ/ρ) is the mass absorption coefficient, which causes the edge structure of the curves.

Quantification using an internal standard can only be applied to residues or thin specimens if troublesome matrix effects do not arise. For this purpose, a critical thickness of 4 μm , 50 nm and 2 nm has to be observed if organic tissues, mineral powders and metallic abrasions, respectively, are investigated.¹⁸

Applications

The particular advantages of high sensitivity, low detection limits and multi-element determination have made TXRF highly applicable for micro-, trace and surface layer

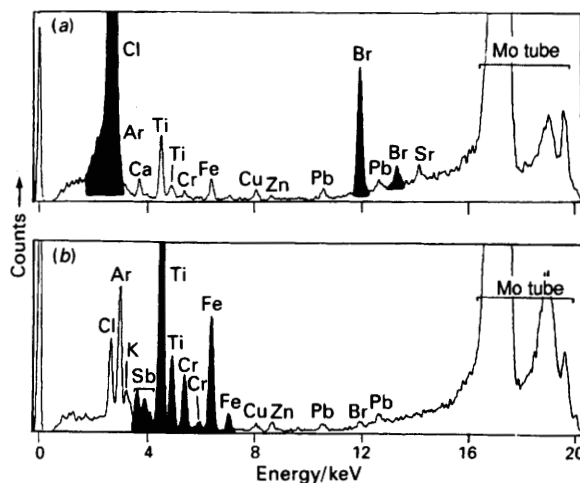


Fig. 8 TXRF spectra of: (a) a crumb of poly(vinyl chloride); and (b) an isolated flake. It becomes clear that the pigment additives TiO_2 and FeO are responsible for the flakes, but not the chalk filler or the lead stabilizer

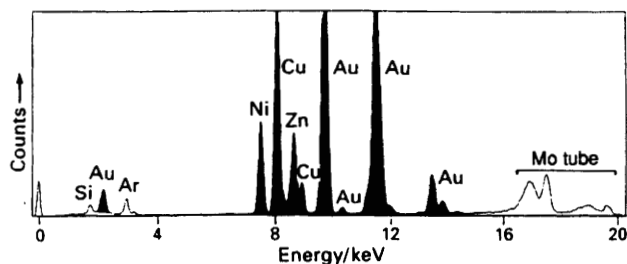


Fig. 9 TXRF spectrum of an ancient golden ring abraded on quartz glass as on a touchstone

analysis. Some examples of these three types of analyses serve to illustrate the capabilities of the method.

Microanalysis

As a method for use in ultra-micro-analysis, TXRF needs only microlitres of solution or suspension or only micrograms of solid or powdered sample. Consequently, all of the techniques and tools for the preparation of minute samples can be used. (i) Single grains, fibres or flakes can be isolated by using a needle or a scalpel and placed on a carrier. If required, a microscope can also be used. The spectra of different particles can be compared, like fingerprints, and key elements identified. An example of trouble shooting is demonstrated in Fig. 8. (ii) Small parts of tissue can be dissected and digested with nitric acid. The solutions can be spiked with an internal standard and analysed. In this way, *in vitro* studies were carried out to investigate the bone formation of incubated periosteal.¹⁹ The uptake of Ca and P was quantitatively determined by TXRF, and furthermore, the amount of hydroxyapatite as the major component of bone was discovered. (iii) The abrasion of metals and alloys is a well-known sampling technique in archaeological measurements and can successfully be applied for TXRF.²⁰ Fig. 9 shows the spectrum of an ancient golden ring that was rubbed on a hard quartz-glass carrier in a single short stroke. Less than 1 μg of the precious specimen was rubbed off, but the major and minor constituents, such as Au, Cu, Ni and Zn, could be detected. By normalizing to 100%, the major constituents could even be determined quantitatively according to

$$c_x = \frac{N_x/S_x}{\sum N_j/S_j} \quad (11)$$

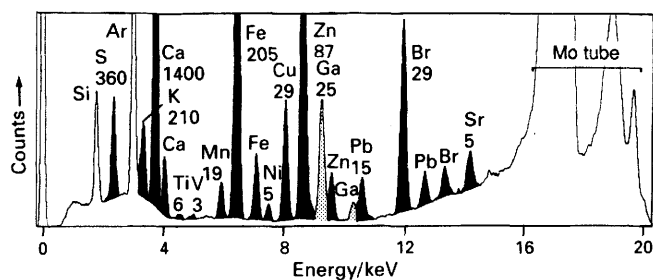


Fig. 10 TXRF spectrum of a droplet of rain water. Gallium was added for internal standardization at 25 ng ml⁻¹. All of the concentration values are given at the ng ml⁻¹ level

The accuracy was estimated by the relative standard deviation to be between 3 and 15%.²⁰

In practice, all rare objects can be analysed in this way, such as precious metals, valuable compounds and specimens available only in limited amounts, which is frequently the case in biology, medicine and criminology. A further category includes inaccessible and irregularly shaped objects which can be abraded on a quartz-glass carrier for subsequent analysis by TXRF.

Trace Analysis

Total reflection X-ray fluorescence spectrometry is ideally suited for ultra-trace analyses, especially of waters or aqueous solutions.²¹ For direct analysis, a few millilitres of the solution are doped with a few microlitres of a standard solution containing a single element (μg ml⁻¹) to serve as an internal standard. Aliquots of 10–50 μl of this solution are deposited on carriers using a microlitre pipette and allowed to dry by means of either a vacuum pump or infrared light. A typical spectrum of rain water spiked with Ga for quantification is shown in Fig. 10. The spectrum shows the K- and L-lines of 14 elements over the range 3–1400 ng ml⁻¹

High-purity acids, such as nitric acid, and organic solvents can be analysed directly, *i.e.*, with no or only little preparation, such as drying. The accuracy of the method can be demonstrated by quantitative analysis of a multi-element standard solution added to nitric acid (with a concentration of 40%). Table 1 shows the results for eight elements determined using Ni as the internal standard (*n*=5). The mean values deviate only a little from the adjusted level of 1 μg ml⁻¹ and the average relative standard deviation is about 3%.

Solid samples are generally analysed after an open-vessel or a pressure digestion. However, finely powdered material can be prepared as a suspension, which is pipetted onto the carriers and analysed directly. Another method of preparing solids is the well-known technique of freeze-cutting,²² which

Table 1 Analysis of a multi-element standard, dissolved in concentrated nitric acid (40%). Nickel was used as the internal standard with a concentration of 2 μg ml⁻¹

Element	Concentration/ μg ml ⁻¹	Mean value (<i>n</i> =5)	RSD (%)
V	1	1.07	4.4
Cr	1	0.95	3.7
Mn	1	1.05	3.3
Fe	1	0.95	2.5
Cu	1	0.95	2.3
Zn	1	1.00	4.2
Ga	1	0.98	2.8
Se	1	1.01	1.9
Mean	1	0.997	3.3

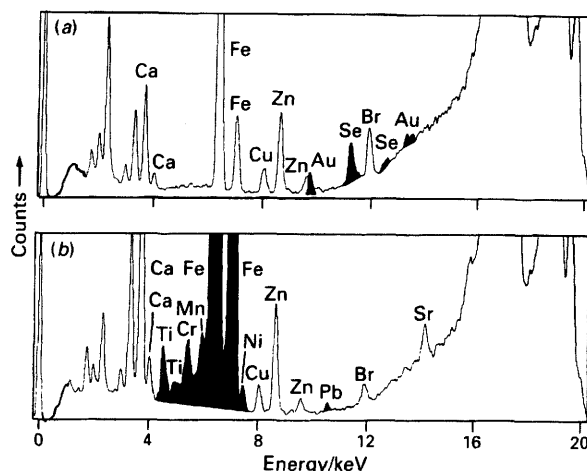


Fig. 11 Spectra of lung tissue showing dust contamination of: (a) a goldsmith; and (b) a foundry worker

is especially suited to biotic samples, solids and fluids. Small pieces of sample are cut by a freezing-microtome and sections of less than 10 μm thickness and 8 mm diameter are placed on carriers for analysis. These sections shrink to the required thickness of about 4 μm by drying. Quantification is performed by simply adding an internal standard prior to analysis and measuring the dry mass after analysis.

As an example, Fig. 11 shows the spectra of pieces of lung tissue taken from a goldsmith and a foundry worker. The bold peaks indicate the distinct presence of Au and Se in the first, and of Ti, Cr, Mn, Fe and Ni in the second case. The deposition at a level of about 100 μg g⁻¹ proves the inhalation of dust particles according to the occupation of different people. As only a few milligrams are needed for sectioning, the method actually presents a micro- and trace analysis method that can be applied to a wide assortment of biological materials.

For a large number of samples, special pre-treatment is needed and even a separation of the matrix might be recommended if still lower detection limits need to be achieved. For ultra-pure fluids, and also rain-water, the freeze-drying technique can be applied, using a sample size of 50 ml. For sea-water, the high portion of salt has to be chemically separated, such as by a reversed-phase technique. For river water, the organic matrix has to be digested prior to analysis. Mineral oils must be substantially diluted with an organic solvent such as tetrahydrofuran. Samples with an organic matrix are preferably ashed prior to analysis.

Table 2 shows the different techniques of sample preparation that are commonly available to analytical chemists. The types of samples analysed after the appropriate preparation steps and the detection limits determined for some elements are also listed.^{29–39} The micro- or even nanogram per litre level can be reached for many samples.

Surface and Surface Layer Analysis

Of course, TXRF is not only suitable for sample material intentionally deposited on optically flat carriers, it can also be used for the determination of contaminant elements on the surfaces of solids, provided these surfaces are optically flat, for example, wafers in the semiconductor industry.^{40,41} The detection limits for the coverage are about 1 × 10¹⁰ atoms cm⁻², which corresponds to 10 ppm of a monolayer.

Furthermore, TXRF is not only suitable for residues or contaminants, which do not reflect the primary beam, but can also be applied for impurities within or beyond a flat surface and for real thin films or layers, which are

Table 2 Detection limits for TXRF analysis of naturally existing samples after appropriate preparation or preconcentration²⁰⁻³⁹

Preparation	Type of sample	Detection limit	Reference
Suspension	Aerosols, dust, ash, suspended matter, sediment	10-100 $\mu\text{g g}^{-1}$	20, 21
	Powdered biomaterial	1-10 $\mu\text{g g}^{-1}$	20
Freeze-cutting	Tissue, foodstuff, biomaterial	0.5-5 $\mu\text{g g}^{-1}$	22
Solution	Mineral oil	1-15 $\mu\text{g ml}^{-1}$	23
	Air dust	0.1-3 $\mu\text{g g}^{-1}$	24
Open digestion	River-water	1-3 ng ml^{-1}	25
	Suspended matter	3-25 $\mu\text{g g}^{-1}$	25
	Fine roots, hair	1-10 $\mu\text{g g}^{-1}$	26, 27
	Blood, serum	20-80 ng ml^{-1}	28
	Ash, mud, soil	5-200 $\mu\text{g g}^{-1}$	29
Pressure digestion	Dust on filter	0.2-6 ng cm^{-2}	30
	Sediment, minerals	15-300 $\mu\text{g g}^{-1}$	25
	Mussel, fish	0.1-1 $\mu\text{g g}^{-1}$	25
	Sediment, mud	1-7 $\mu\text{g g}^{-1}$	31
	Hay (powder)	0.2-2 $\mu\text{g g}^{-1}$	26
Drying	Rain- and river-water	0.1-3 ng ml^{-1}	26, 32
	High-purity acids	5-50 pg ml^{-1}	33, 34
Freeze-drying	Drinking-, rain-water	20-100 pg ml^{-1}	25, 32
	High-purity water	$\approx 1 \text{ pg ml}^{-1}$	27
Ashing	Digested fine roots	0.1-1 $\mu\text{g g}^{-1}$	26
	Aerosols on filter	0.6-20 ng cm^{-2}	30
	Blood serum	40-220 ng ml^{-1}	35
Chemical matrix separation	Rain-, sea-water	3-20 pg ml^{-1}	25, 31, 32, 36
	Digested river-water	50-500 pg ml^{-1}	25
	Digested blood	2-30 ng ml^{-1}	28, 35
	Digested aluminium	5-20 ng g^{-1}	37
	Digested iron	30-140 ng g^{-1}	38
	Digested Si and SiO ₂	10-200 ng g^{-1}	39
	Sulfuric acid	1-200 ng ml^{-1}	39

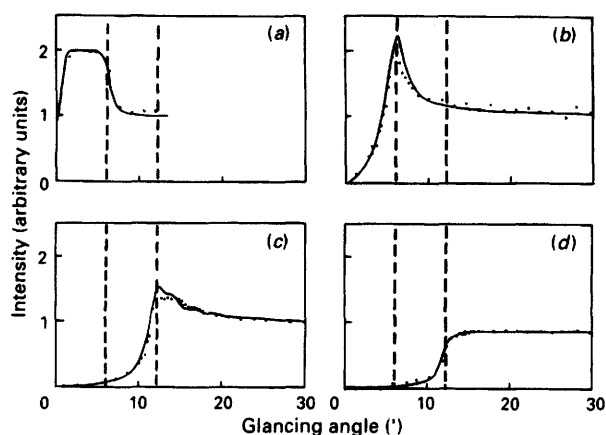


Fig. 12 Angle-dependent intensity profiles of different thin films applied to a silicon wafer.⁴⁹ (a) Br residue; (b) 1 nm Co film; (c) 30 nm Co film; and (d) 100 nm Co film. (Glancing angle given in minutes)

are themselves totally reflecting.⁴²⁻⁴⁹ For a detailed investigation, however, angle-dependent intensity profiles have to be recorded. The glancing angle has to be varied between 3 and 50 min with a resolution of about 0.1 min. Instruments with the required characteristics are commercially available.

The different capabilities of angle-dependent TXRF are illustrated in Fig. 12.⁴⁹ A residue of Br (a) shows the doubled line intensity below the critical angle. According to eqn. (4), the critical angle for Mo $K\alpha$ -radiation striking a silicon substrate, amounts to about 6 min. This behaviour is

already known from Fig. 3. A completely different profile is recorded for a reflecting Co film of 1 nm thickness [Fig. 12 (b)]. A maximum is formed that results from the standing wave generated by the interference of the incident and the reflected beam. The corresponding peak, with more than doubled intensity, appears at the critical angle of silicon, which is still decisive.

If the thickness of the Co film is increased to 30 nm [Fig. 12 (c)], the peak maximum is reduced and its position is shifted to 12 min. This angle corresponds to the critical angle of Co and is determined by the changed density ($\rho = 8.92 \text{ g cm}^{-3}$ instead of 2.33 g cm^{-3}).

The last curve [Fig. 12 (d)] represents a Co layer of 100 nm thickness. The intensity profile now approximates the profile of the bulk material. A similar but shifted profile can be recorded from Co impurities within an Si layer.

Generally, important information can be received from the recorded profiles. The components of a thin film or layer can be determined in addition to the thickness of the layer. Furthermore, the location of impurities can be found. Impurities in a residue can be distinguished from those in a reflecting film or a substrate, and finally the density (ρ) of a surface layer can be determined. These studies can even be expanded from single to multiple thin-films.^{49,50} However, up until now rectangular profiles have to be assumed for this type of non-destructive depth profiling. Currently, applications are aimed at characterizing the cleaning and deposition procedures, such as metallization, coating and implantation of wafers, provided that they are optically flat and still unstructured.

Conclusion

Owing to a number of considerable benefits, the novel method of TXRF has achieved a remarkable strength.

One particular advantage of the method is the possibility of analysing various types of sample although only specimens of limited mass and thickness have to be prepared. Above all, TXRF is suitable for ultra-microanalysis requiring only a minute amount of sample, $<10\ \mu\text{l}$ for liquids and $<1\ \mu\text{g}$ for solids. A consumption-free operation enables the same sample to be analysed repeatedly. The multi-element capability includes about 80 elements, excluding the lightest elements. The simultaneous determination of up to 20 elements in practice is just as remarkable as the time-saving operation.

The high detection power for heavier elements is the most outstanding feature, making the method suitable for ultra-trace analysis. In this respect, TXRF can compete very well with established methods such as atomic absorption spectrometry, neutron activation analysis or inductively coupled plasma optical emission spectrometry, which has been proven by round-robin tests performed by the International Atomic Energy Agency.⁵¹ Unfortunately, the light elements with atomic numbers of <11 (Na) are either undetectable or have high detection limits. A simple and reliable quantification by the addition of a single internal standard can be recommended. The high precision and accuracy satisfy the most stringent analytical requirements, although sampling errors can arise in a combined trace- and microanalysis, which, in general, are unavoidable. Obviously, TXRF requires a dust-free operation on a 'clean-bench'.

A new field of applications has been opened for surface and surface layer analysis by non-destructive depth profiling in the region of up to 100 nm. No vacuum is needed, no charging problems arise and the samples remain undamaged. In relation to conventional spectrometers, the instrumentation is simple and inexpensive. However, only optically flat samples such as wafers can be investigated. The composition, thickness, position and even the density of the thin films or layers can be determined. The detection power for contamination equals the capability of secondary ion mass spectrometry. The lateral resolution is limited, but a focus of some micrometres is reached if a synchrotron is used for excitation.^{43,47}

Generally, the advantages make TXRF suitable for a great number of analytical problems. At the moment, TXRF is employed at only about 40 locations world-wide, but an analytical breakthrough is expected to evolve in the near future.

References

- 1 Yoneda, Y., and Horiuchi, T., *Rev. Sci. Instr.*, 1971, **42**, 1069.
- 2 Aiginger, H., and Wobrauschek, P., *Nucl. Instrum. Methods*, 1971, **114**, 157.
- 3 Wobrauschek, P., and Aiginger, H., *Anal. Chem.*, 1975, **47**, 852.
- 4 Knoth, J., Schwenke, H., Marten, R., and Glauer, J., *J. Clin. Chem. Clin. Biochem.*, 1977, **15**, 557.
- 5 Knoth, J., and Schwenke, H., *Fresenius Z. Anal. Chem.*, 1978, **291**, 200.
- 6 Knoth, J., and Schwenke, H., *Fresenius Z. Anal. Chem.*, 1980, **301**, 7.
- 7 *Totalreflexions-Röntgenfluoreszenzanalyse*, eds. Michaelis, W., and Prange, A., GKSS-Forschungszentrum, Geesthacht, 1987, pp. 7-98.
- 8 Boumans, P. W. J. M., and Klockenkämper, R., eds., *Spectrochim. Acta, Part B*, 1989, **44**, pp. 433-549.
- 9 Boumans, P. W. J. M., Wobrauschek, P. and Aiginger, H., eds., *Spectrochim. Acta, Part B*, 1991, **46**, pp. 1313-1436.
- 10 Schwenke, H., Berneike, W., Knoth, J., and Weisbrod, U., *Adv. X-ray Anal.*, 1989, **32**, 105.
- 11 Schwenke, H., and Knoth, J., *Nucl. Instrum. Methods*, 1982, **193**, 239.
- 12 Freitag, K., Reus, U., and Fleischhauer, J., *Spectrochim. Acta, Part B*, 1989, **44**, 499.
- 13 Iida, A., and Gohshi, Y., *Jpn. J. Appl. Phys.*, 1984, **23**, 1543.
- 14 Reus, U., Freitag, K., Haase, A., and Alexandre, J. F., *Spectra* 2000, 1989, **143**, 42.
- 15 Strelci, C., Aiginger, H., and Wobrauschek, P., *Spectrochim. Acta, Part B*, 1989, **44**, 491.
- 16 Wobrauschek, P., Kregsamer, P., Strelci, C., and Aiginger, H., *X-ray Spectrom.*, 1991, **20**, 23.
- 17 Freitag, K., in *Instrumentelle Multielement-Analyse*, ed. Sansoni, B., VCH, Weinheim, 1985, p. 257.
- 18 Klockenkämper, R., and von Bohlen, A., *Spectrochim. Acta, Part B*, 1989, **44**, 461.
- 19 Niemann, A., von Bohlen, A., Klockenkämper, R., and Keck, E., *Biochem. Biophys. Res. Commun.*, 1990, **170**, 1216.
- 20 von Bohlen, A., Eller, R., Klockenkämper, R., and Tölg, G., *Anal. Chem.*, 1987, **59**, 2551.
- 21 Michaelis, W., Knoth, J., Prange, A., and Schwenke, H., *Adv. X-ray Anal.*, 1985, **28**, 75.
- 22 von Bohlen, A., Klockenkämper, R., Tölg, G., and Wiecken, B., *Fresenius Z. Anal. Chem.*, 1988, **331**, 454.
- 23 Bilbrey, D. B., Leland, D. J., Leyden, D. E., Wobrauschek, P., and Aiginger, H., *X-ray Spectrom.*, 1987, **16**, 161.
- 24 Leland, D. J., Bilbrey, D. B., Leyden, D. E., Wobrauschek, P., and Aiginger, H., *Anal. Chem.*, 1987, **59**, 1911.
- 25 Prange, A., Knoth, J., Stöbel, R.-P., Böttdeker, H., and Kramer, K., *Anal. Chim. Acta*, 1987, **195**, 275.
- 26 Prange, A., *GIT Fachz. Lab.*, 1987, **6**, 513.
- 27 Prange, A., *Spectrochim. Acta, Part B*, 1989, **44**, 437.
- 28 Prange, A., Böttdeker, H., and Michaelis, W., *Fresenius J. Anal. Chem.*, 1990, **335**, 914.
- 29 Gerwinski, W., and Goetz, D., *Fresenius Z. Anal. Chem.*, 1987, **327**, 690.
- 30 Ketelsen, P., and Knöchel, A., *Fresenius Z. Anal. Chem.*, 1984, **317**, 333.
- 31 Knöchel, A., Diercks, H., Hastenteufel, S., and Haurand, M., *Fresenius Z. Anal. Chem.*, 1989, **334**, 673.
- 32 Stöbel, R.-P., and Prange, A., *Anal. Chem.*, 1985, **57**, 2880.
- 33 Reus, U., Freitag, K., and Fleischhauer, J., *Fresenius Z. Anal. Chem.*, 1989, **334**, 674.
- 34 Prange, A., Kramer, K., and Reus, U., *Spectrochim. Acta, Part B*, 1991, **46**, 1385.
- 35 Knöchel, A., Bethel, U., and Hamm, V., *Fresenius Z. Anal. Chem.*, 1989, **334**, 673.
- 36 Prange, A., Knöchel, A., and Michaelis, W., *Anal. Chim. Acta*, 1985, **172**, 79.
- 37 Burba, P., Willmer, P.-G., Becker, M., and Klockenkämper, R., *Spectrochim. Acta, Part B*, 1989, **44**, 525.
- 38 Chen, J. S., Berndt, H., Klockenkämper, R., and Tölg, G., *Fresenius J. Anal. Chem.*, 1990, **338**, 891.
- 39 Reus, U., *Spectrochim. Acta, Part B*, 1989, **44**, 533.
- 40 Penka, V., and Hub, W., *Spectrochim. Acta, Part B*, 1989, **44**, 483.
- 41 Berneike, W., Knoth, J., Schwenke, H., and Weisbrod, U., *Fresenius Z. Anal. Chem.*, 1989, **333**, 524.
- 42 Iida, A., Sakurai, K., Yoshinaga, A., and Gohshi, Y., *Nucl. Instrum. Methods*, 1986, **A246**, 736.
- 43 Iida, A., Sakurai, K., and Gohshi, Y., *Adv. X-ray Anal.*, 1988, **31**, 487.
- 44 Hoffmann, P., Zieser, K. H., Hein, M., and Flakowski, M., *Spectrochim. Acta, Part B*, 1989, **44**, 471.
- 45 Eichinger, P., Rath, H. J., and Schwenke, H., *ASTM Spec. Tech. Publ.*, 1989, **990**, 305.
- 46 Knoth, J., Schwenke, H., and Weisbrod, U., *Spectrochim. Acta, Part B*, 1989, **44**, 477.
- 47 Sakurai, K., and Iida, A., *Adv. X-ray Anal.*, 1990, **33**, 205.
- 48 Weisbrod, U., Gutschke, R., Knoth, J., and Schwenke, H., *Fresenius J. Anal. Chem.*, 1991, **341**, 83.
- 49 de Boer, D. K. G. and van den Hoogenhof, W. W., *Spectrochim. Acta, Part B*, 1991, **46**, 1323.
- 50 Weisbrod, U., Gutschke, R., Knoth, J., and Schwenke, H., in the press.
- 51 Michaelis, E., *Fresenius Z. Anal. Chem.*, 1986, **324**, 662.

Paper 1/02951G
Received June 18, 1991
Accepted July 22, 1991